

Accepted Manuscript

Real time monitoring of glucose in whole blood by smartphone

Miguel M. Erenas, Belén Carrillo Aguilera, Kevin Cantrell, Sara Gonzalez-Chocano, Isabel Perez de Vargas Sansalvador, Ignacio de Orbe-Payá, Luis Fermin Capitan-Vallvey



PII: S0956-5663(19)30309-4

DOI: <https://doi.org/10.1016/j.bios.2019.04.024>

Reference: BIOS 11256

To appear in: *Biosensors and Bioelectronics*

Received Date: 6 February 2019

Revised Date: 22 March 2019

Accepted Date: 12 April 2019

Please cite this article as: Erenas, M.M., Aguilera, Belé.Carrillo., Cantrell, K., Gonzalez-Chocano, S., de Vargas Sansalvador, I.P., de Orbe-Payá, I., Capitan-Vallvey, L.F., Real time monitoring of glucose in whole blood by smartphone, *Biosensors and Bioelectronics* (2019), doi: <https://doi.org/10.1016/j.bios.2019.04.024>.

This is a PDF file of an unedited manuscript that has been accepted for publication. As a service to our customers we are providing this early version of the manuscript. The manuscript will undergo copyediting, typesetting, and review of the resulting proof before it is published in its final form. Please note that during the production process errors may be discovered which could affect the content, and all legal disclaimers that apply to the journal pertain.

Real time monitoring of glucose in whole blood by smartphone

Miguel M. Erenas*^{1,2}, Belén Carrillo Aguilera¹, Kevin Cantrell³, Sara Gonzalez-Chocano¹, Isabel Perez de Vargas Sansalvador^{1,2}, Ignacio de Orbe-Payá^{1,2} and Luis Fermin Capitan-Vallvey^{1,2}

¹ ECsens. Department of Analytical Chemistry. ² Unit of Excellence in Chemistry applied to Biomedicine and the Environment of the University of Granada. Campus Fuentenueva, Faculty of Sciences, 18071, University of Granada, Spain.

³ Department of Chemistry. The University of Portland, 5000 N Willamette Blvd, Portland, OR 97203, USA.

Abstract

A combined thread-paper microfluidic device (μ TPAD) is presented for the determination of glucose in blood. The device is designed to include all the analytical operations needed: red blood cell separation, conditioning, enzymatic recognition, and colorimetric transduction. The signal is captured with a smartphone or tablet working in video mode and processed by custom Android-based software in real-time. The automatic detection of the region of interest on the thread allows for the use of either initial rate or equilibrium signal as analytical parameters. The time needed for analysis is 12 s using initial rate, and 100 s using the equilibrium measurement with a LOD of 48 μ M and 12 μ M, respectively, and a precision around 7%. The μ TPAD allows a rapid determination of glucose in real samples using only 3 μ L of whole blood.

*Corresponding author, email: erenas@ugr.es

Keywords: Thread-paper microfluidic device; Glucose determination; Whole blood; Reaction rate; Smartphone.

41 **1. Introduction**

42 In our global society there is a drive to move the acquisition of chemical information
43 from the controlled environments of labs to the place where the information is needed.
44 This necessitates changing the methods used to generate analytical information from
45 approaches that are instrument and lab centered, to decentralized user-centered
46 approaches, the so-called distributed approaches (Hoekstra et al., 2018). One type of
47 analytical system that has the potential to provide fast, laboratory-quality results is lab-
48 on-a-chip devices that rely on microfluidic platforms allowing the miniaturization of
49 chemical assays (Mark et al., 2010). The use of capillarity as a liquid propulsion
50 principle presents advantages over other more complex propulsion systems in terms of
51 simplicity, low cost, biocompatibility, fast response, and user-friendly format. The
52 development of devices based mainly on paper, thread, and cloth have evolved into an
53 active research field with an increasing number of publications and reviews (Akyazi et
54 al., 2018;Aydingogan et al., 2018;Farajikhah et al., 2019;Hoekstra et al., 2018;Li and
55 Steckl, 2018).

56 In combination with consumer electronic devices that include color sensors, mainly
57 smartphones and tablets, capillary-based devices have the potential to become a total
58 analytical system. These total analytical systems must be considered as a whole and
59 include everything needed to perform the analysis: sampling, sample treatment,
60 conditioning, analyte recognition, measurements, electronic equipment, and data
61 processing. They should operate in the most robust and simple way possible. These
62 systems do not produce data, but information relevant to the user in an understandable
63 format.

64 The use of thread brings various advantages for the manufacture of analytical devices in
65 terms of definition of path, strength, varied materials, and small volume of samples
66 (Nilghaz et al., 2013). Thread has been used as support for the manufacture of
67 microfluidic devices (μ TAD) that can implement various analytical operations, such as
68 support for recognition (Wu et al., 2016) and transduction reactions (Liu et al., 2017),
69 immobilization of reagents (Galpothdeniya et al., 2014), chromatographic (Agustini et
70 al., 2018) or electrophoretic (Cabot et al., 2018) separations, control and manipulation
71 of flow (Ballerini et al., 2011;Li et al., 2018) or sample conditioning (Ulum et al.,
72 2016). The measurement techniques are mainly optical and electrochemical, by
73 integrating electrodes onto the thread (Malon et al., 2017). The most commonly used
74 optical measurements, apart from the visual ones, are based on the acquisition of images

75 from the device with a scanner (Mao et al., 2015) or with a smartphone (Erenas et al.,
76 2016) and subsequent processing.

77 A variant in the design of microfluidic devices consists of the combination of thread and
78 paper which gives rise to the so-called microfluidic thread-paper based analytical device
79 (μ TPAD). These devices developed mainly by the team of Prof. F.A. Gómez, combine
80 the good conduction of fluids by the thread with the recognition process and the
81 subsequent acquisition of the color information from an image of a paper area obtained
82 with a scanner. They have been used for the enzymatic determination of glucose using a
83 three-channel system made with nylon thread and three reaction areas of
84 chromatographic paper (Gonzalez et al., 2016; Lee et al., 2018). Other systems described
85 include a 3D multilayered paper μ TPAD for the determination of glucose and BSA
86 (Neris et al., 2019) and two ELISA for biotinylated goat anti-mouse IgG and rabbit IgG
87 (Gonzalez et al., 2018a; Gonzalez et al., 2018b). Sateanchok et al. (Sateanchok et al.,
88 2018) describes a μ TPAD together with a smartphone for the total phenolic content in
89 green tea using a thread portion for the handling of samples and a paper portion for
90 reaction with immobilized reagents.

91 In this paper we consider the acquisition of the color information of the microfluidic
92 device through a smartphone working in video mode. This opens the door to use kinetic
93 measures to obtain analytical information, which can significantly shorten the analysis
94 time. Additionally, the determination of glucose in whole blood requires separating the
95 red blood cell (RBC) from the plasma, which is achieved with an μ TPAD incorporating
96 a separation membrane. Blood samples collected from volunteers were analyzed with
97 μ TPAD as well as with a portable glucose meter, in order to validate results.

98

99 **2. Experimental methods**

100 **2.1 Materials and Equipment.** The thread used as support for the μ TPAD preparation
101 was a commercial white cotton thread (caliber 12 and NTex 94) from Finca (Presencia
102 Hilaturas S.A. Alzira, Valencia, Spain) measuring around 600 μ m in diameter and
103 containing 250 ± 10 fibers (Erenas et al., 2016). The reagents included on the thread were
104 3,3',5,5'-tetramethylbenzidine (TMB), glucose oxidase from *Aspergillus Niger* (GOx),
105 horseradish peroxidase (HRP), chitosan, β -D-glucose, and phosphate buffer solution
106 (1xPBS) containing NaCl, KCl, Na_2HPO_4 and KH_2PO_4 . All these reagents were
107 purchased from Sigma Aldrich (Sigma–Aldrich Quimica S.A., Madrid, Spain). Acetic
108 acid, ethanol, and hydrogen peroxide were purchased from Panreac S.A. (Barcelona,

109 Spain). Reverse osmosis type quality water (Milli-RO 12 plus Milli-Q station
110 (Millipore, Bedford, MA, U.S.), conductivity 18.2 M Ω ·cm) was used throughout.
111 Whole blood separation membranes MF1, LF1, VF2 and GF/DVA were used and
112 purchased from Whatman (Little Chalfont, Buckinghamshire, United Kingdom).
113 All the blood samples were obtained from healthy volunteers and collected in tubes
114 containing EDTA to avoid the clotting of samples. Once the blood samples were
115 extracted they were preserved at 4°C for up to one week.
116 The μ TAD images were recorded and processed using a variety of devices including a
117 Sony DSC-HX300 digital camera (Sony, Tokyo, Japan), a Samsung Galaxy S5
118 smartphone, a Samsung Galaxy Tab A tablet (Samsung Electronics, Suwon, South
119 Korea), and a Motorola Moto G4 Play smartphone (Lenovo Goup LTD, Beijing,
120 China). ImageJ software (National Institutes of Health, Bethesda, Maryland, USA) with
121 the Color Space Converter plugin ([http://rsb.info.nih.gov/ij/plugins/color-space-](http://rsb.info.nih.gov/ij/plugins/color-space-converter.html)
122 [converter.html](http://rsb.info.nih.gov/ij/plugins/color-space-converter.html)) was used to analyze digital images. Avidemux 2.6 (Mean) was used to
123 obtain single frames from video files for analysis by ImageJ. The Anaconda distribution
124 of Python (Continuum Analytics), OpenCV (Open Source Computer Vision), and
125 Android Studio (Google) were used for the development of application software for the
126 processing of video files and for the real-time Android app.
127 The laboratory evaluations of glucose μ TAD in whole blood and plasma samples were
128 completed for validation purposes using an Accu-Chek Aviva Nano glucose meter
129 (Roche, Switzerland) provided with test-strips.

130

131 **2.2 Thread-based device preparation**

132 The outer waxy layer of cotton thread, called cuticle, confers hydrophobic properties
133 which affects the wicking and wetting properties. To remove this layer, the thread is
134 scoured in a boiling solution of 10 mg/mL Na₂CO₃ for 5 minutes (Nilghaz and Shen,
135 2015). Afterwards, the thread is washed several times until the rinsate has a neutral pH,
136 sonicated 3 times in purified water for 5 minutes, allowed to dry at room temperature,
137 and stored in a closed container for further use.

138 The basic design of the μ TAD for glucose determination is shown in Figure 1i. It
139 consists of a 2.5 cm-long thread attached to a piece of double-sided adhesive tape with
140 three different regions: A) a sampling region where sample is placed; B) a recognition
141 region where GOx is retained and H₂O₂ produced; and C) a transduction region where
142 TMB is oxidized changing the color of thread (Scheme S2). To prepare the device, 5.0

143 μL of 1xPBS is added in the sampling region and allowed to dry for two minutes. Then
144 1.0 μL of 1.74 U/ μL GOx is added in the recognition region followed by 0.35 μL of
145 20.8 mM TMB in ethanol, 0.35 μL of $3.5 \cdot 10^{-2}$ U/mL HRP, and, after waiting one
146 minute, 0.7 μL of a 1 mg/mL chitosan aqueous solution is added to the transduction
147 region. The device is then left to dry at room temperature for a few minutes. The
148 devices are kept in the darkness until use.

149 Figure 1
150 For whole blood glucose determination, the μTAD preparation was modified for the
151 small volume of serum produced (Figure 1ii). To a 1.5 cm-long piece of thread 2.5 μL
152 of 1xPBS is added to the sampling region and allowed to dry at room temperature for 10
153 minutes. Then 0.5 μL of a solution containing $2.8 \cdot 10^{-2}$ U/mL HRP, 3.48 U/mL GOx,
154 0.5 μL of 14.56 mM TMB in ethanol, and 0.7 μL of 1 mg/mL chitosan in water is
155 deposited in the recognition and transduction region. Finally, a 4 mm x 5 mm diameter
156 tear-shaped piece of LF1 whole blood separation membrane was placed at the beginning
157 of sampling region of thread.

158 In order to use the μTAD for whole blood glucose determination we designed a two-
159 piece methacrylate custom case (Figure 1iii) that holds the thread in a channel engraved
160 for this purpose and allows the acquisition of video with the smartphone. The case was
161 designed using Illustrator software and engraved using a Rayjet Trotec Laser engraving
162 printer (Trotec, Austria) using Rayjet Commander software. A thread and separation
163 membrane are placed on the groove in the bottom piece, and the top, that has two holes
164 for sampling and recording the video, is placed over it, and the μTAD is ready for use.

165

166 **2.3 μTAD image capture and processing**

167 The digital images were captured using a Sony DSC-HX300 digital camera and
168 Motorola Moto G⁴ Play smartphone. For still images the camera was set-up as follows:
169 resolution of 3648x2736 pixels, aperture value f/3.5, exposure time 1/40 s, ISO-80,
170 2800K white balance (see Figure S1), and images were saved in jpg format (Joint
171 Photographic Experts Group). For video recordings the camera was set-up as follows:
172 resolution of 1440x1080 pixels, 25 frames per second, and 2800K white balance, and
173 the files were saved in MTS (AVCHD) format. All the images and videos were captured
174 inside a custom cubic light box illuminated by two LED light bulbs (3000K) located in
175 a fixed position. Image and video files from the μTAD were analyzed using ImageJ and
176 the in-house app. All the optimization related to the μTAD and μTPAD , was performed

177 using the Sony digital camera to image the device. Calibration and validation of the
178 device was performed using Motorola Moto G⁴ Play smartphone and the custom
179 Android app.

180

181 **2.4 Developed software for image-processing**

182 The basic steps employed in the custom image processing software are outlined here,
183 and a more detailed description is given in the supplementary information. The image
184 is first transformed from the RGB color space to the HSV color space. The hue channel
185 is used to identify the type of pixel (e.g. red pixels are whole blood; blue pixels are
186 chemically active areas of the thread), and the saturation channel is used to identify the
187 region of interest and track the degree of color development. An additional set of values,
188 the color absorbance ratios, are also calculated. These three values, hereafter referred to
189 as cA123, are defined as the negative log of the ratio of two RGB channels. For
190 example, cA1 is the $-\log(\text{Blue}/\text{Green})$ (Cantrell et al., 2010). A single region of interest
191 (ROI) was automatically identified as the largest contiguous group of colored pixels.
192 Pixels are masked as colored if their saturation is greater than a threshold amount (≥ 40
193 in an 8-bit image). Only pixels inside this ROI are used in subsequent data
194 manipulations. For pixels in the ROI, the mean, median, and standard deviation are
195 calculated for RGB, HSV, and cA123, and a histogram of the individual values is
196 displayed on the screen and recorded in a text file along with the elapsed time for that
197 frame. A subset of the data from 12 seconds before the elapsed time up to and including
198 the current frame is defined. A least-squares linear fit to the analytical parameter versus
199 time within the 12s window is then calculated. The slope of this line is taken to be the
200 rate of change in the device response. Both the moving average of the analytical
201 parameter and the rate of change are displayed as separate auto-scaling plots. The raw
202 video, processed video, and summary data for each frame are each stored as separate
203 files. The Android-based application was developed and tested using two different
204 Samsung devices. The final calibration and validation of the μ TPAD was done with a
205 lower processing capacity Motorola Moto G⁴ Play smartphone.

206

207 **2.5 Calibration and validation of μ TAD and μ TPAD**

208 In order to use the μ TPAD, 3 μ L of whole blood sample was deposited on the sampling
209 area, and a Motorola Moto G⁴ Play smartphone running the Android-based app was
210 used to monitor the color change. To validate the results, the concentrations obtained

211 were compared to a commercial glucometer (Accu-Check) together with the glucose
212 test strips. The test-strip is introduced in the glucometer, and 0.6 μL of whole blood is
213 placed on the sampling area to measure the glucose concentration with the glucometer.
214 Each whole blood sample was analyzed 3 times using the glucometer and results
215 obtained compared to the provided by the μTPAD in terms of percent error.

216

217 **3. Results and discussion**

218 Thread is a potential substrate for microfluidic devices fabrication with some
219 advantages compared to paper such as high mechanical strength (both in dry and wet
220 conditions), flexibility, lightweight, and ease of functionalization. A large variety of
221 materials with different properties are available, and the thread itself is the driving
222 channel, contrary to what happens in paper in which the channel must be defined
223 (Malon et al., 2017; Nilghaz et al., 2013). A very common substrate is cotton, a super-
224 hydrophilic material, whose specific properties depend on chemical composition and
225 surface morphology (Darmanin and Guittard, 2014). In this application, the gaps intra-
226 yarn, inter-yarn, and lumen of each fiber account for the capillary action by wicking the
227 liquid into the thread (Banerjee et al., 2013). We selected commercial cotton thread
228 ($\sim 600 \mu$ diameter and 250 ± 10 fibers) as the material for the capillary platform combined
229 with paper to implement all analytical operations: particles separation, fluid transport,
230 chemistry immobilization and colorimetric transduction. The capillary movement of
231 water in the selected thread shows minor deviation from Washburn-type behavior ($L = a$
232 \sqrt{t} ; $a = 0.8185 \pm 0.0065$). The μTAD designed for glucose determination is a single-
233 channel device with a sampling area on one end of the thread and a detection area
234 containing the recognition chemistry at the other end. The principle of the dry-reagent
235 cotton thread-based assay is based on enzymatic oxidation of glucose using GOx/HRP
236 and colorimetric transduction with TMB.

237

238 **3.1 μTAD optimization**

239 To adjust the enzymatic solution method to the μTAD format, different variables were
240 studied and optimized (additional details are given in the supplementary information).
241 For the transduction reactions the on-thread TMB immobilization, the amount of TMB
242 and HRP, and the pH adjustment were all optimized. For the recognition reactions the
243 amount of GOx and volume of sample added were studied. TMB is the reagent selected
244 for the optical transduction of the enzymatically generated H_2O_2 . TMB is insoluble in

245 water, but the blue oxidation product is soluble and can be dragged through the medium
246 by the sample. Chitosan is used to preconcentrate the oxidized TMB in the detection
247 area as it is strongly retained to paper (Ariza-Avidad et al., 2016; Gabriel et al., 2016)
248 and cloth-based devices (Bagherbaigi et al., 2014). It slows the movement of the
249 oxidized TMB and increases the homogeneity of the ROI (Liu et al., 2014). The
250 deposition of 0.7 μg of chitosan (0.7 μl of 1 mg/mL solution) reduces the length of
251 TMB oxidized area (16%) and improves reproducibility (from 20.3% CV without
252 chitosan to 3.6% with it, $n=3$) (Table S1).

253 As TMB and HRP mutually influence one another, their optimization was performed
254 simultaneously by a factorial design obtaining a maximum saturation signal for 14.0 μU
255 and $7.3 \cdot 10^{-3}$ μmol of HRP and TMB, respectively (Figure S3). The immobilization by
256 drying of pH 7.4 PBS buffer in the thread improves the precision (7.6% compared to
257 11.5%) and simplifies the use of the device, thus we included the buffer in the μTAD
258 although it reduces the equilibrium value of the saturation signal (Figure S4).

259 To study the GOx dependence, different concentrations were deposited on the thread
260 and the evolution of saturation signal was monitored over time (Figure S5). The largest
261 saturations were obtained with 1.74 U of GOx. Interestingly a substantial lowering in
262 the reaction time for equilibration (100 s) was observed, which is a much lower time
263 than described in literature, typically around 10 min (Table S3).

264 The maximum saturation signal was obtained for 10 μL samples. For smaller volumes,
265 the signal decreases because a smaller amount of glucose is present, and the precision is
266 lower due to the thread not being completely wet (Figure S6). Alternatively, at higher
267 sample volumes the oxidized TMB is dragged from ROI, decreasing the signal and
268 lowering the precision.

269

270 **3.2 μTAD analytical characterization**

271 To study the performance of the system we prepared 10 different glucose standards, five
272 replicates each, using 50 different μTAD devices (each is a one-use device) while
273 recording the evolution of colors with a smartphone in real-time using the custom
274 Android app. As analytical parameters we studied both the initial reaction rate using a
275 window of 12 s from the time when the app detects a change on the color of thread
276 (Figure 2) and the equilibrium signal measured as the saturation 100 seconds after the
277 sample addition (Figure S7). In both cases, the relationship between the logarithm of

278 glucose concentration and the analytical parameter is sigmoidal and is fitted to a
279 Boltzmann equation (Equation 1).

280

$$281 \quad y = A_2 + \frac{(A_1 - A_2)}{1 + e^{-\frac{(x - A_3)}{A_4}}} \quad \text{Eq. 1}$$

282

Figure 2

283 Analytical figures of merit obtained using both methods (rate based and equilibrium)
284 are shown in Table 1. The limit of detection was calculated as 6 times the standard
285 deviation of the blank (Mistberger et al., 2014), obtaining a value of 48 μM for initial
286 rate and 12 μM when equilibrium saturation is used. These values are much lower than
287 those in the literature for colorimetric μPAD 's for glucose (Chun et al., 2014; Gabriel et
288 al., 2017; Gonzalez et al., 2016) and comparable to those obtained by a bipolar ECL
289 thread-based method (Liu et al., 2017) (Table S3). A precision study was also
290 performed at three different concentrations, 10 replicates each, obtaining values ranging
291 from 5.5% to 7.8%. Although an analysis time of 100 seconds is a major improvement
292 for colorimetric devices compared with literature (Ariza-Avidad et al., 2016; Gabriel et
293 al., 2017; Zhu et al., 2017), the use of initial rate measured in real-time further reduces
294 the analysis time down to 12 seconds. A study of the stability of μTAD over time in two
295 different preservation conditions, fridge and desiccator, showed short lifetimes (Figure
296 S8) as is typical for these systems (Zhu et al., 2017).

297

Table 1

298 **3.3 Glucose determination in whole blood**

299 To perform the conventional spectrophotometric determination of glucose in blood in
300 the laboratory, it is necessary to separate plasma from the RBC via centrifugation, to
301 avoid their interference in the blue color of oxidized TMB (Li and Steckl, 2018). In
302 order to meet the ASSURED guidelines (Mabey et al., 2004), we studied the inclusion
303 of an RBC separation step in the developed μTAD while keeping the device as small as
304 possible.

305 Different strategies have been described in literature to integrate RBC separation from
306 plasma in paper and thread devices. Some are based on the use of different salts in the
307 thread to induce blood clotting, such as NaCl (Nilghaz and Shen, 2015; Yan et al., 2014)
308 or CaCl_2 (Li et al., 2014); anticoagulants such as EDTA (Ulum et al., 2016);
309 agglutinating antibodies (Al-Tamimi et al., 2012; Yang and Lin, 2015) or paper
310 membranes (Songjaroen et al., 2012).

311 The use of NaCl or EDTA in different conditions of concentration and temperature did
312 not result in appreciable separation of plasma in the small volumes of blood used (see SI
313 3.8). Blood filter paper (Songjaroen et al., 2012) is used to separate the RBC from
314 whole blood by trapping them on the membrane while allowing plasma to flow by
315 capillarity to the recognition area. As paper filters to remove particles greater than 2–3
316 μm , we tested polyvinyl alcohol-bound glass fiber membranes (MF1, LF1 and VF2) and
317 binder-free glass fiber membrane (VF1). To test filter papers, a 6 mm round shape
318 membrane was located at the beginning of the μTAD and 10 μL of whole blood was
319 used. Only LF1 paper provided a sufficient amount of plasma for samples this small.
320 To reduce the blood volume needed, we designed a tear shape membrane connected to
321 the thread by the tip (Figure 1ii) and tested different tear sizes and blood volumes. We
322 selected a 4 mm x 5 mm diameter tear-shaped membrane and 3 μL of blood. Figure 3
323 shows the plot-line saturation profiles of the device with 3 μL and 4 μL of blood. A
324 sharp change in saturation is observed for the 3 μL sample size indicating better RBC
325 separation than the progressive increase seen in the 4 μL sample size.

Figure 3

327 Due to the low volume of plasma obtained from 3 μL of whole blood, it was necessary
328 to redesign the device to overlap the recognition and detection areas (Figure 1ii).
329 Consequently, we designed a combined thread – paper microfluidic device, a μTPAD ,
330 to include the different analytical operations needed for glucose analysis in total blood:
331 RBC separation, conditioning, recognition, and transduction.

332 For ease the use, we designed a custom casing in two-piece methacrylate. The bottom is
333 engraved with a slit that allows lodging both the thread and the membrane in a fixed
334 position. The top has two holes for sampling and collecting the signal with the
335 smartphone (Figure S4). This housing was designed to fulfill the ASSURED guidelines
336 of user-friendly operation and safety; the user cannot touch the sampling area or thread
337 where the reaction will occur.

338 To calibrate the μTPAD a series of whole blood samples with known amounts of
339 glucose around physiological levels were prepared. A 50 μL aliquot of whole blood was
340 left at room temperature for 6 hours so that glycolysis consumes the glucose present,
341 and it was then spiked with 0.5 μL of a glucose standard. The calibration function is
342 shown in Figure 4, and the details of the fit to linear equation and figures of merit are
343 presented in Table 1. Due to the rapid change in color of the μTPAD when a whole
344 blood sample is analyzed, it is not possible to use the initial rate as analytical parameter.

345
346 A precision study was carried out at 50.0, 90.0 and 110.0 mg/dL of glucose, with 10
347 replicates per solution. Relative standard deviations of 6.6%, 6.9% and 5.2%,
348 respectively, were measured. Taking into account that the precision of the colorimetric
349 method in a laboratory is around 5% (Burtis and Bruns, 2007), the values obtained with
350 this device are quite acceptable. This complete system not only measures the glucose
351 concentration, but it also separates plasma from whole blood and performs multiple
352 buffered reactions without any manipulation of sample. Finally, the price of a sensor
353 was estimated to be 0.0087 €/μTPAD without the case and 0.0999 €/μTPAD including
354 it. (Table S2).

355 Once the development and optimization of the different variables were performed, a
356 study of interference species was carried out (Section 3.1 in the SI) and finally, the
357 μTPAD was applied to real whole blood samples supplied from seven different healthy
358 volunteers. In all cases, 3 μL of blood was added to the μTAD without any kind of
359 previous treatment. The measured values range from 3% to 17% (Table 2) percent error
360 when compared to a commercial glucose meter.

361

362 **4. Conclusions**

363

364 This study develops the first colorimetric microfluidic-based procedure combined with
365 a smartphone app to obtain kinetic or equilibrium signals in real time. The procedure is
366 implemented in a microfluidic single-channel device that combines cotton thread and
367 paper, μTPAD, for glucose analysis in whole blood with no need for any pre-treatment.
368 The combination of several analytical operations, such as buffering, and the separation
369 of the red blood cells from the plasma, along with the use of thread as the support
370 simplifies the operational procedure and reduces the analysis time. The analytical
371 approach shown here can be extended to the real-time monitoring of a variety of
372 chemicals or biomarkers by selecting the type of procedure (kinetic/equilibrium),
373 depending on the concentration of the analyte in combination with capillary
374 microfluidic devices. This strategy opens the way to the simple application of kinetic
375 procedures using a smartphone, increasing the versatility of ready-to-use procedures.

376 The main limitation of the presented procedure is related to the short lifetime of the
377 μTPAD device, due to the loss of activity of the enzymatic material. Future work will
378 focus on replacing enzymes with nanozymes or including enzymes in co-embedded
379 flower-like nanomaterials to improve the lifetime of the device, as well as developing

380 kinetic procedures for on-site detection based on processing information captured with a
381 smartphone video camera and thread-based devices.

382

383 **Acknowledgements**

384 This study was supported by the CTQ2016-78754-C2-1-R project from the Spanish
385 MINECO.

386

387 **References**

388 Agustini, D., Fedalto, L., Bergamini, M.F., Marcolino-Junior, L.H., 2018. *Lab Chip* 18,
389 670-678.

390 Akyazi, T., Basabe-Desmonts, L., Benito-Lopez, F., 2018. *Anal.Chim.Acta* 1001, 1-17.

391 Al-Tamimi, M., Shen, W., Zeineddine, R., Tran, H., Garnier, G., 2012. *Anal.Chem.* 84,
392 1661-1668.

393 Ariza-Avidad, M., Salinas-Castillo, A., Capitan-Vallvey, L.F., 2016. *Biosensors*
394 *Bioelectron.* 77, 51-55.

395 Aydindogan, E., Guler Celik, E., Timur, S., 2018. *Anal.Chem.* 90, 12325–12333.

396 Bagherbaigi, S., Corcoles, E.P., Wicaksono, D.H.B., 2014. *Anal.Methods* 6, 7175-
397 7180.

398 Ballerini, D.R., Li, X., Shen, W., 2011. *Biomicrofluidics* 5, 014105-1-014105/13.

399 Banerjee, S.S., Roychowdhury, A., Taneja, N., Janrao, R., Khandare, J., Paul, D., 2013.
400 *Sens.Actuators B* 186, 439-445.

401 Burtis, A. C., Edwrd, R., Bruns, E. D., 2008. *Fundamentals of Clinical Chemistry :6th*
402 *Ed, Building. Elsevier.*

403 Cabot, J.M., Breadmore, M.C., Paull, B., 2018. *Anal Chim Acta* 1000, 283-292.

404 Cantrell, K., Erenas, M.M., Orbe-Paya, I., Capitan-Vallvey, L.F., 2010. *Anal.Chem.* 82,
405 531-542.

406 Chun, H.J., Park, Y.M., Han, Y.D., Jang, Y.H., Yoon, H.C., 2014. *BioChip J.* 8, 218-
407 226.

408 Darmanin, T., Guittard, F., 2014. *Prog.Polym.Sci.* 39, 656-682.

409 Erenas, M.M., de Orbe-Paya, I., Capitan-Vallvey, L.F., 2016. *Anal.Chem.* 88, 5331-
410 5337.

411 Farajikhah, S., Cabot, J.M., Innis, P.C., Paull, B., Wallace, G.G., 2019. *ACS Comb.Sci.*

412 Gabriel, E.F.M., Garcia, P.T., Cardoso, T.M.G., Lopes, F.M., Martins, F.T., Coltro,
413 W.K.T., 2016. *Analyst* 141, 4749-4756.

414 Gabriel, F.E., Garcia, T.P., Lopes, M.F., Coltro, K.W., 2017. *Micromachines* 8, 104.

- 415 Galpothdeniya, W.I., McCarter, K.S., De Rooy, S.L., Regmi, B.P., Das, S., Hasan, F.,
416 Tagge, A., Warner, I.M., 2014. RSC Adv. 4, 7225-7234.
- 417 Gonzalez, A., Estala, L., Gaines, M., Gomez, F.A., 2016. Electrophoresis 37, 1685-
418 1690.
- 419 Gonzalez, A., Gaines, M., Gallegos, L.Y., Guevara, R., Gomez, F.A., 2018a.
420 Electrophoresis 39, 476-484.
- 421 Gonzalez, A., Gaines, M., Gallegos, L.Y., Guevara, R., Gomez, F.A., 2018b. Methods
422 146, 58-65.
- 423 Hoekstra, R., Blondeau, P., Andrade, F.J., 2018. Anal.Bioanal.Chem. 410, 4077-4089.
- 424 Lee, W., Gonzalez, A., Arguelles, P., Guevara, R., Gonzalez-Guerrero, M.J., Gomez,
425 F.A., 2018. Electrophoresis 39, 1443-1451.
- 426 Li, H., Han, D., Pauletti, G.M., Steckl, A.J., 2014. Lab Chip 14, 4035-4041.
- 427 Li, H., Steckl, A.J., 2018. Anal.Chem. 91, 352-371.
- 428 Li, Y.D., Li, W.Y., Chai, H.H., Fang, C., Kang, Y.J., Li, C.M., Yu, L., 2018. Cellulose
429 25, 4831-4840.
- 430 Liu, R., Liu, C., Li, H., Liu, M., Wang, D., Zhang, C., 2017. Biosensors Bioelectron. 94,
431 335-343.
- 432 Liu, W., Yang, H., Ding, Y., Ge, S., Yu, J., Yan, M., Song, X., 2014. Analyst 139, 251-
433 258.
- 434 Mabey, D., Peeling, R.W., Ustianowski, A., Perkins, M.D., 2004. Nat.Rev.Microbiol. 2,
435 231.
- 436 Malon, R.S.P., Heng, L.Y., Corcoles, E.P., 2017. Rev.Anal.Chem. 36, 1-19.
- 437 Mao, X., Du, T.E., Meng, L., Song, T., 2015. Anal.Chim.Acta 889, 172-178.
- 438 Mark, D., Haerberle, S., Roth, G., von Stetten, F., Zengerle, R., 2010. Chem.Soc.Rev.
439 39, 1153-1182.
- 440 Mistberger, G., Crespo, G.A., Bakker, E., 2014. Annu.Rev.Anal.Chem. 7, 483-512.
- 441 Neris, N.M., Guevara, R.D., Gonzalez, A., Gomez, F.A., 2019. Electrophoresis 40,
442 296-303.
- 443 Nilghaz, A., Ballerini, D.R., Shen, W., 2013. Biomicrofluidics 7, 51501.
- 444 Nilghaz, A., Shen, W., 2015. RSC Adv. 5, 53172-53179.
- 445 Sateanchok, S., Wangkarn, S., Saenjum, C., Grudpan, K., 2018. Talanta 177, 171-175.
- 446 Songjaroen, T., Dungchai, W., Chailapakul, O., Henry, C.S., Laiwattanapaisal, W.,
447 2012. Lab Chip 12, 3392-3398.
- 448 Ulum, M.F., Maylina, L., Noviana, D., Wicaksono, D.H.B., 2016. Lab Chip 16, 1492-
449 1504.

450 Wu, T., Xu, T., Xu, L.P., Huang, Y., Shi, W., Wen, Y., Zhang, X., 2016.
451 Biosens.Bioelectron. 86, 951-957.

452 Yan, C., Yu, S., Jiang, Y., He, Q., Chen, H., 2014. Huaxue Xuebao 72, 1099-1104.

453 Yang, Y.A., Lin, C.H., 2015. Biomicrofluidics 9, 022402-1-022402/12.

454 Zhu, X., Huang, J., Liu, J., Zhang, H., Jiang, J., Yu, R., 2017. Nanoscale 9, 5658-5663.
455
456
457
458
459
460
461
462
463
464
465
466
467
468
469
470
471
472
473
474
475
476
477
478
479
480
481
482
483
484
485
486
487
488
489
490
491
492
493
494
495
496
497
498
499
500
501
502
503
504
505
506

507
508
509
510
511
512
513
514
515
516
517
518
519
520
521
522
523
524
525
526

Table 1. Calibration function and analytical parameter of the method when saturation and initial rate are used as analytical parameter.

Calibration function (Initial rate)		Calibration function (Saturation)		Calibration function (Total blood)	
A1	-0.006	A1	0.164		
A2	3.352	A2	0.776	Intercept	5.344
A3	2.666	A3	2.403	Slope	0.257
A4	0.320	A4	0.490		
R ²	0.987	R ²	0.966	R ²	0.991
LOD	48 μ M	LOD	12 μ M	LOD	28 mg/dL
Analysis time	12 s	Analysis time	100 s	Analysis time	~10 s
Precision (n=10)					
15 μ M	10.2 %	15 μ M	7.8 %	50 mg/dL	6.6%
125 μ M	5.7 %	125 μ M	7.2 %	90 mg/dL	6.9 %
500 μ M	9.1 %	500 μ M	5.5 %	110 mg/dL	5.2 %

527
528
529
530
531
532
533
534
535
536
537
538
539
540
541
542
543
544

545
546
547
548
549
550
551
552
553
554
555
556
557
558

559

560

561
562
563
564
565

Table 2. Validation of whole blood samples using the μ TPAD and a commercial glucose meter as reference method.

Whole blood sample	Glucose meter	μ TPAD	Error
1	65 mg/dL	67 mg/dL	3%
2	66 mg/dL	72 mg/dL	10%
3	51 mg/dL	60 mg/dL	17%
4	65 mg/dL	59 mg/dL	10%
5	73 mg/dL	75 mg/dL	3%
6	119 mg/dL	113 mg/dL	5%
7	67 mg/dL	79 mg/dL	4%

566
567
568
569
570
571
572
573
574
575
576
577
578
579
580
581
582
583
584
585

586
587
588
589
590
591
592
593
594
595
596
597
598
599
600
601
602
603
604
605
606
607
608
609
610
611
612
613
614
615
616
617
618
619
620

Figures

Figure 1. i) Picture of the μ TAD for glucose: A) Sampling region; B) detection region; C) transduction region. ii) Picture of μ TPAD for whole blood glucose: D) RBC paper based separation membrane and sampling area; E) detection and transduction area. iii) Case designed to contain the μ TPAD with a hole for blood sampling and a window for video recording.

Figure 2. Calibration of μ TAD sensing membrane using initial rate and adjust to a Boltzmann equation.

Figure 3. Saturation (S) plot profile of the device when different volumes of 3 and 4 μ L of whole blood sample are added. i) 3 μ L; ii) 4 μ L.

Figure 4. Calibration (n=5) of μ TPAD obtained from whole blood spiked samples using saturation (S) as analytical parameter.

621

622

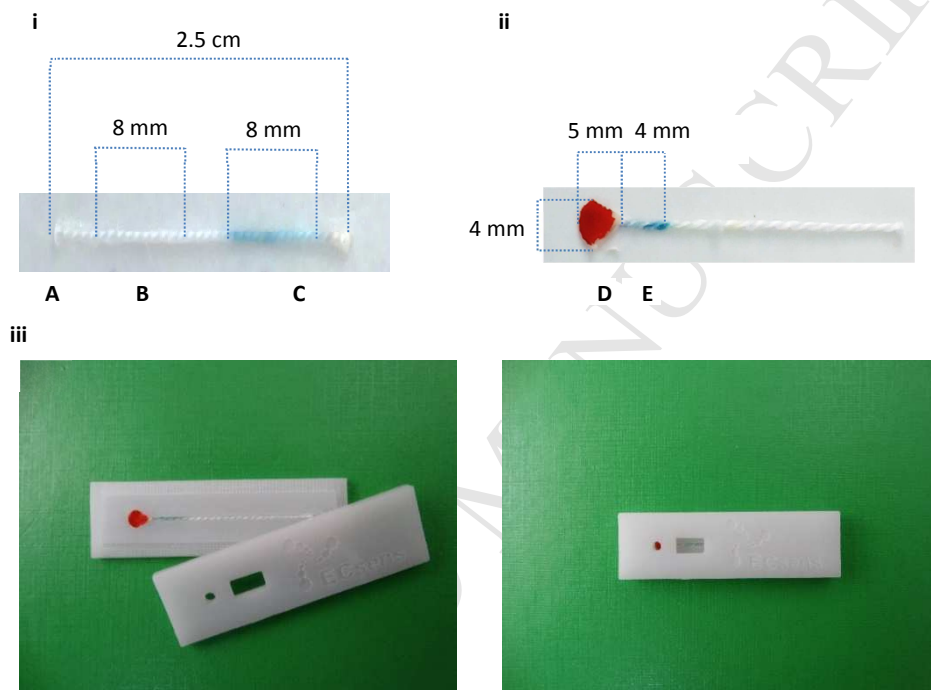
623

624

625

626

627



628

629

630

631

632

633

634

635

636

637

638

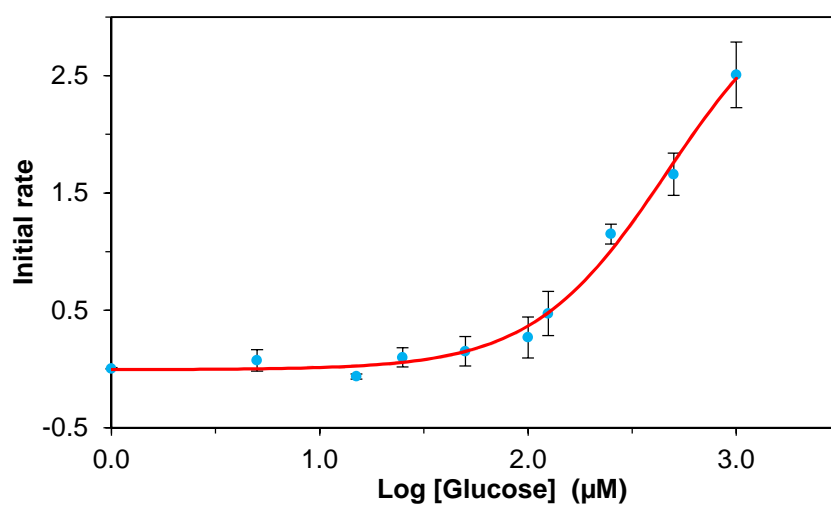
639

640

641

Figure 1

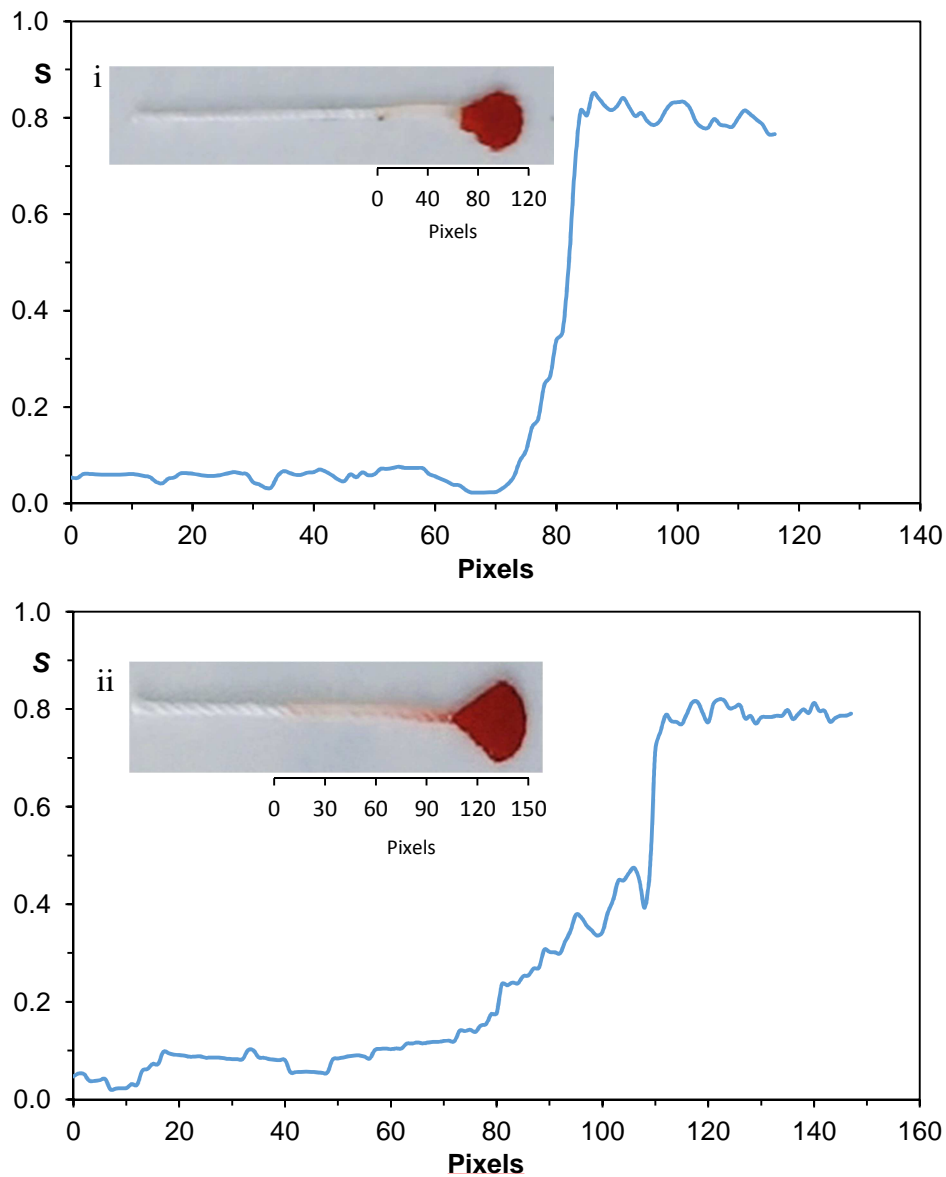
642
643
644
645
646
647
648
649
650
651
652
653
654



655
656
657
658
659
660
661
662
663
664
665
666
667
668
669
670
671

Figure 2

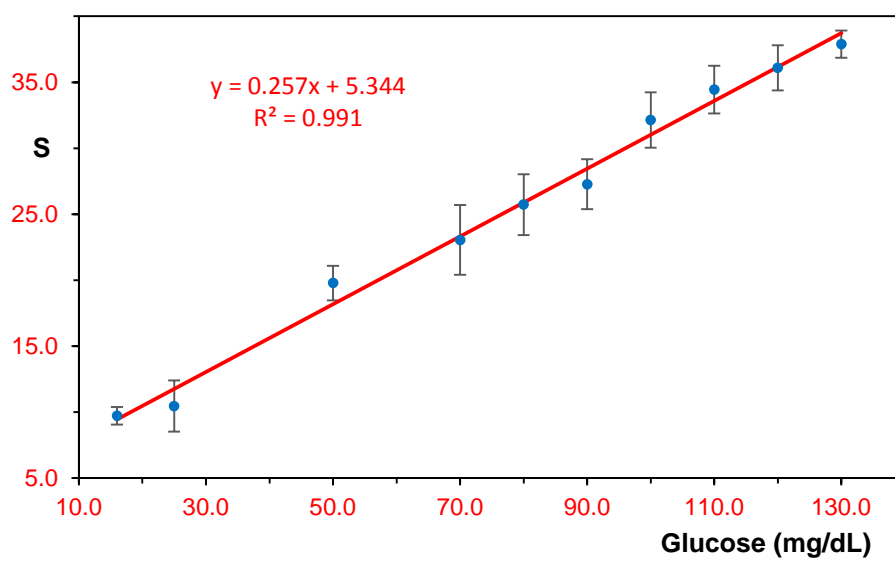
672
673
674
675
676



677
678
679
680
681
682
683
684
685
686
687
688

Figure 3

689
690
691
692
693
694
695
696
697



698
699
700
701
702

Figure 4

Highlights

- A μ TPAD for the determination of glucose in whole blood has been developed using 3 μ L of sample.
- The device include analytical operations needed: red blood cell separation, sample conditioning, enzymatic recognition, and colorimetric transduction.
- An Android based app permit the automatic detection of the ROI on the thread allowing for the use of either initial rate or equilibrium signal as analytical parameters.

Declaration of interests

The authors declare that they have no known competing financial interests or personal relationships that could have appeared to influence the work reported in this paper.

The authors declare the following financial interests/personal relationships which may be considered as potential competing interests: